JOURNAL OF MATERIALS SCIENCE 18 (1983) 1604–1614

Mode III and Mode I fatigue crack propagation behaviour under torsional loading

E. K. TSCHEGG
Technical University of Vienna, Institute of Applied and Technical Physics, A-1040 Vienna, Karlsplatz 13, Austria

Fatigue crack growth rates have been measured under cyclic torsional loading ($R = -1$, 1 Hz loading frequency) in AISI 4340 steel tempered at 650° C, with circumferentially-notched specimens (12.7 mm specimen diameter). The Mode III fatigue crack growth curve for macroscopically flat fracture surface – being obtained by an extrapolation procedure which eliminates the "Mode III crack closure" influence – has higher crack growth rates and shows a greater slope than Mode I results in the stress intensity range of $\Delta K_{\text{IIIeff}} = 18$ to 50 MPa $m^{1/2}$. In the range of $\Delta K_{\text{IIIeff}} < 18$ MPa $m^{1/2}$, the fracture surface has "factory roof" morphology (Mode I). The difference between fatigue crack growth behaviour in Mode III and Mode I as well as mechanisms that can lead to a fracture mode change are discussed. A comparison of the Mode III crack closure influence for specimen diameters of 12.7 mm (this study) and of 24.5 mm (an earlier study) shows that this influence is not only dependent on the depth of the crack and applied torque but also on the specimen diameter. The extrapolated crack growth rates show good agreement with measurements for various specimen diameters.

Nomenclature

a	uncracked ligament of circumferentially-notched specimen containing a crack.
b	external diameter of circumferentially-notched specimen.
c	crack length emanating from the notch root.
$(\Delta c/\Delta N)_i$	fatigue crack growth rate in Mode i = I, III.
CTD_I	crack tip diplacement in Mode I.
ΔCTD_i	cyclic crack tip displacement in Mode i = I, III.
E	elastic modulus.
G	shear modulus.
k	monotonic shear yield strength.
K_i	stress intensity factor for Mode i = I, III.
ΔK_I	alternating cyclic stress intensity factor in Mode I.
ΔK_{IIIeff}	effective alternating stress intensity in Mode III.
ΔK_{IIInom}	nominal alternating stress intensity in Mode III.
ΔK_{ith}	threshold stress intensity for crack growth in Mode i = I, II, III.
P	applied axial load.
R	ratio of minimum to maximum load or torque.
$r_{\Delta i}$	cyclic plastic zone size for Mode i = I, III.
T	applied torque.
UTS	ultimate tensile strength.
Y	monotonic yield strength in tension.

1. Introduction

In the last ten years, the understanding of fatigue crack growth in metallic materials in the crack opening mode (Mode I) has increased enormously through intensive research in this field. This has brought about a reduction in catastrophic engineering failures and a significant improvement in techniques for the estimation of the remaining lifetime of pre-cracked components. For fatique, in an antiplane shear mode (often the case with shafts in machines and in power plants), few investigations on Mode III have been carried out in

0022–2461/83 $03.00 + .12

comparison with the amount of published research on Mode I.

A complex condition in Mode III crack growth is that the crack is closed during the Mode III loading. Friction, abrasion, and mutual support increasingly reduce the efficiency of the applied torque with increasing crack length, i.e. the effective torque experienced at the crack tip. Thus, the effective cyclic stress intensity value (ΔK_{IIIeff}) experienced at the crack tip is reduced from the nominally applied value (ΔK_{IIInom}). This "Mode III crack closure" influence was first investigated, qualitatively and quantitatively, on notched shafts of AISI 4340 steel [1, 2]. Based on these results, further investigations were conducted on notched shafts of softer materials as well [3, 4]. Earlier studies on notched steel shafts of AISI 4340 [5] and EN 16 steel [6] as well as on notched, three-finger plate specimens of 6061-T6 aluminium [7] in Mode III stressing have not considered this influence and obtained fatigue crack propagation rates smaller by a factor of 10 to 50 than Mode I crack growth at the same nominal stress intensity range [5, 6]. Mode III threshold values of [6] are a factor of about two larger than Mode I values.

Measurements were conducted [8] on shafts of 24.5 mm diameter from AISI 4340 steel, tempered at 650° C, with circumferential notch, at constant ΔK_{IIInom}, and the crack growth rates at the different constant ΔK_{IIInom} were plotted as a function of crack length c. A monotonic decrease of the crack propagation rate showed at all measured constant ΔK_{IIInom} values in the region of 30 to 60 MPa $m^{1/2}$ at a crack depth of 0.4 to 4 mm. When a crack propagation rate of approximately 5×10^{-5} mm (cycle)$^{-1}$ was reached, the macroscopically flat fracture surface changed to the "factory-roof" type fracture.* By extrapolation of the $(\Delta c/\Delta N)_{\text{III}}$ against c-curves to a crack length of $c = 0$ (= crack length emanating from the notch root), crack growth propagation rates could be estimated which are considered not to be influenced by "Mode III crack closure". The crack growth curve ($\log (\Delta c/\Delta N)_{\text{III}}$ against $\log \Delta K_{\text{IIInom}}$) derived from these values was linear in the range 30 to 60 MPa $m^{1/2}$ and lies above the Mode I crack growth curve. The Mode III curve furthermore has a larger slope than that for Mode I. It is supposed [8] that at smaller stress intensity values, the branch cracks forming at the crack tips in Mode I grow faster than the mean Mode III crack and that fracture of the "factory roof" type is thus introduced.

With this in mind, the aim of this study is now to investigate the change of fracture mode and thus the value of the Mode III threshold. Furthermore, an attempt is made to study the influence of the "Mode III crack closure" on the crack growth behaviour in Mode III while reducing the specimen's diameter to one half that of [8].

TABLE I Composition of AISI 4340 steel in wt %

C	Mn	Ni	Cr	Mo	Si	P	S	Cu
0.4	0.78	1.77	0.81	0.25	0.26	0.07	0.013	0.14

2. Material and experimental procedure

The steel selected for this study was AISI 4340. Its chemical composition is reported in Table I. The steel was heat treated by austenitizing at 870° C for 1 h followed by oil quenching and tempering at 650° C for 1 h. The mechanical properties are summarized in Table II. The shear yield strength was calculated as $k = Y/3^{1/2}$.

The fatigue tests were performed on cylindrical specimens with a diameter of 12.7 mm and a length between the grips of 35 mm. After the heat treatments, a circumferential starter notch was cut into the centre of the specimens (notch depth 0.631 mm, angle 60° and notch radius <0.015 mm).

Tests were performed in torque control (rotary motion), and load control (linear motion) on an automated Instron servohydraulic torsion-tension testing machine at a frequency of 1 Hz (sine wave) and with zero mean torque ($R = -1$). The testing condition was 20° C in laboratory air.

Crack lengths were monitored using the d.c. potential drop technique in a continuous measurement process. Details on the calibration procedures and the use of this technique are described in [9, 10].

A small axial load was applied during the

TABLE II Room temperature mechanical properties of AISI 4340 steel (austenitized at 870° C, oil quench, tempered at 650° C)

Tensile yield strength monotonic	$Y = 956$ MPa
Ultimate tensile strength	UTS = 1076 MPa
Shear yield strength monotonic	$k = Y/3^{1/2} = 552$ MPa

*Cracks oriented at 45° to the specimen axis; crack advances occur in crack opening mode (Mode I).

TABLE III Equation list for Mode I and Mode III calculations

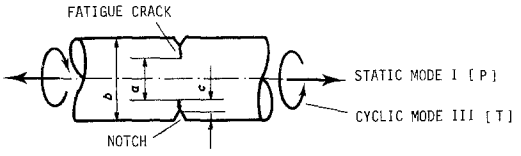

Mode I	Mode III
$K_I = \frac{2^{1/2}P}{\pi a^2}[\pi a(1-a/b)]^{1/2} f(a/b)$	$K_{III} = 3(2)^{1/2}\frac{T}{\pi a^3}[\pi a(1-a/b)]^{1/2} g(a/b)$
$f(a/b) = 1 + 0.5a/b + 0.375(a/b)^2 - 0.363(a/b)^3 + 0.731(a/b)^4$	$g(a/b) = 1 + 0.5a/b + 0.375(a/b)^2 + 0.313(a/b)^3 + 0.273(a/b)^4 + 0.208(a/b)^5$
$r_{\Delta I} = \frac{1}{2\pi}\left(\frac{\Delta K_I}{2Y}\right)^2$	$r_{\Delta III} = \frac{1}{\pi}\left(\frac{\Delta K_{III}}{2k}\right)^2$
$\Delta CTD_I \sim \frac{1}{2}\frac{\Delta K_I^2}{2YE} \sim \frac{2\pi Y}{E} r_{\Delta I}$	$\Delta CTD_{III} \sim \frac{2}{\pi}\frac{\Delta K_{III}^2}{2kG} \sim \frac{4k}{G} r_{\Delta III}$

All equations for small-scale yielding condition.

measuring procedure so that a constant static K_I value of 3 MPa $m^{1/2}$ acted at the crack tip in order to make the crack length measurement more accurate and reproducible [10].

The values for stress intensity ($K_{I, III}$), plastic zone size ($r_{\Delta I, III}$) and crack tip displacement ($\Delta CTD_{I, III}$) were calculated according to correlations reported in the literature [11–13] for small scale yielding conditions. These equations are listed in Table III.

The tests were performed in "stress intensity control". That is, the stress intensity value ΔK_{IIInom} at the crack tip was held constant during the test. This implies that the applied torque is to be determined from the measured crack length and by a defined constant ΔK_{IIInom} value. This procedure was applied for $\Delta K_{IIInom} = 15$, 20, 25, 30 MPa $m^{1/2}$.

The specimens were precracked to a crack length of 0.2 mm with a torque of 160 Nm for the test with $\Delta K_{IIInom} = 20$, 25, 30 MPa $m^{1/2}$ and 130 Nm for the test with $\Delta K_{IIInom} = 15$ MPa $m^{1/2}$. The tests were stopped when the crack depth reached a value of 0.8 mm. The specimens were then removed from the machine, cooled down to liquid N_2 temperature and fractured by bending impact [14].

Early studies [2] have shown that if precracking occurred symmetrically along the notch root, final fracture was concentric with the centre of the specimen. The diameter of the final fracture was used to provide a running check of the calibration in the electrical potential crack monitor.

3. Results

3.1. Fractography

Crack initiation in all specimens exhibited a macroscopically flat fracture mode. For tests with constant $\Delta K_{IIInom} = 20$, 25, 30 MPa $m^{1/2}$, the fatigue crack continued in this fracture mode to a crack depth of 0.8 mm, at which the measurements ended. Fig. 1 shows a typical picture of a macroscopically flat fracture mode, depicting a

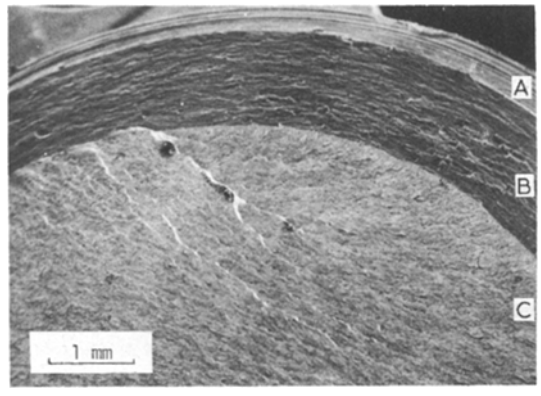

Figure 1 Fractography of a typical pure Mode III fracture surface at $\Delta K_{IIInom} = 20$ MPa $m^{1/2}$ (produced in "stress intensity control") in AISI 4340 steel tempered at 650° C. (From top to bottom: notch (A) – macroscopically flat Mode III fatigue fracture (B) – impact final fracture at LN_2 (C)).

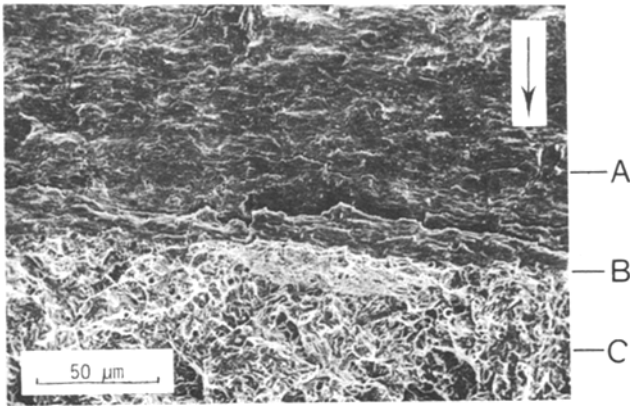

Figure 2 Detail of Fig. 1 showing branch cracks near the crack tip. (Mode III fatigue fracture surface – A, fatigue crack tip – B, impact final fracture at LN_2 – C). Arrow shows the crack growth direction.

sector of a specimen after fatigue at $\Delta K_{\mathrm{IIInom}} = 20\,\mathrm{MPa\,m^{1/2}}$. A detail of this, enlarged 500 times, is shown in Fig. 2, exhibiting the fracture surface in the area of the fatigue crack tip. The fatigue crack surface is microscopically rough and textured with numerous radially as well as tangentially running branching cracks. These branch cracks in Mode III + II and Mode I can also be found close to the fatigue crack tip, as seen in Fig. 2. In the test with constant $\Delta K_{\mathrm{IIInom}} = 15\,\mathrm{MPa\,m^{1/2}}$, the fatigue crack changes after the crack initiation into the "factory roof" fracture mode (Mode I). In Fig. 3, a sector of the fracture is shown. Fig. 4 shows a detail of Fig. 3, in which the growth of the fatigue crack in Mode I can be recognized by flow lines on the 45° inclined sloping "roof". The initiation of the factory roof crack can be usually found in Mode III + II branch cracks, which depart so much from the mean crack that they could be described as part of a surface of a truncated cone (cone axis = specimen's axis). The upper part of Fig. 5 shows the mean Mode III crack, which proceeds to become a Mode III + II branch crack toward the middle of the picture. The Mode I crack start and continuation are well recognizable by the patterns on the "roofs".

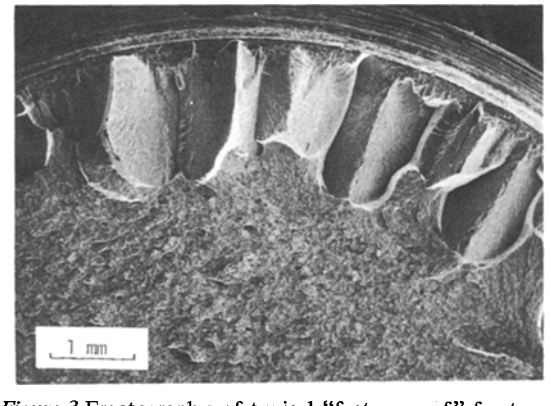

Figure 3 Fractography of typical "factory roof" fracture surface at $\Delta K_{\mathrm{IIInom}} = 15\,\mathrm{MPa\,m^{1/2}}$ (produced in "stress intensity control") in AISI 4340 tempered at 650°C. (From top to bottom: notch – fatigue crack initiation – fatigue crack in Mode III – "factory roof" fracture surface – impact final fracture at LN_2 temperature.)

3.2. Fatigue crack growth measurements

The crack growth rates measured on the 12.7 mm diameter specimens are plotted in Fig. 6 as a function of crack length c. With the loading condition in "stress intensity control", the fatigue crack should grow with constant crack growth rates. However, through the influence of the "Mode III crack closure", the crack growth rates decrease with growing crack length at all constant $\Delta K_{\mathrm{IIInom}}$ values. Evidence for abrasion and friction are given by the fact that black spherical shaped iron powder particles are found on the fracture surface after the test, and red α–Fe_2O_3 powder has been observed to squeeze out from the crack during the test. This has been reported to be typical for abra-

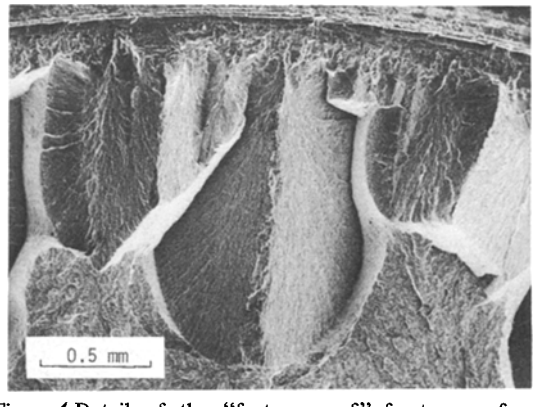

Figure 4 Detail of the "factory roof" fracture surface shown in Fig. 3. Note the flow lines on the roofs, indicating Mode I crack propagation.

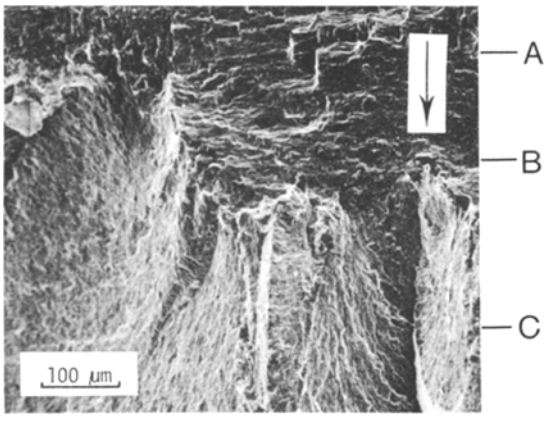

Figure 5 Fractography of transition at $\Delta K_{IIInom} = 15\,MPa\,m^{1/2}$ from Mode III type to "factory roof" fatigue fracture. (From top to bottom: main Mode III fatigue crack – A, Mode III + II branch crack – B, "factory roof" crack – C). Arrow shows the main crack growth direction.

sion [15]. For specimens with 12.7 mm diameter, this was much less noticeable than that in the studies of [8] on 24.5 mm diameter specimens. The results shown in Fig. 6 also indicate that the reduction of fatigue crack propagation rates with increasing crack length for the 24.5 mm diameter specimen (dash-dot lines in Fig. 6) show a larger negative slope than the results of this study. In contrast to this is the measurement with constant $\Delta K_{IIInom} = 15\,MPa\,m^{1/2}$, for which the fatigue crack grew in a "factory-roof" mode. From the interlocking of the "factory roofs" during loading we can understand why the crack growth rate, which reduces itself greatly with increasing crack length, cannot be compared with values for macroscopically flat fatigue cracks.

If an extrapolation of the measured curves in Fig. 6 to a crack length of $c = 0$ (indicated by fine dashed lines) is conducted, estimations of crack

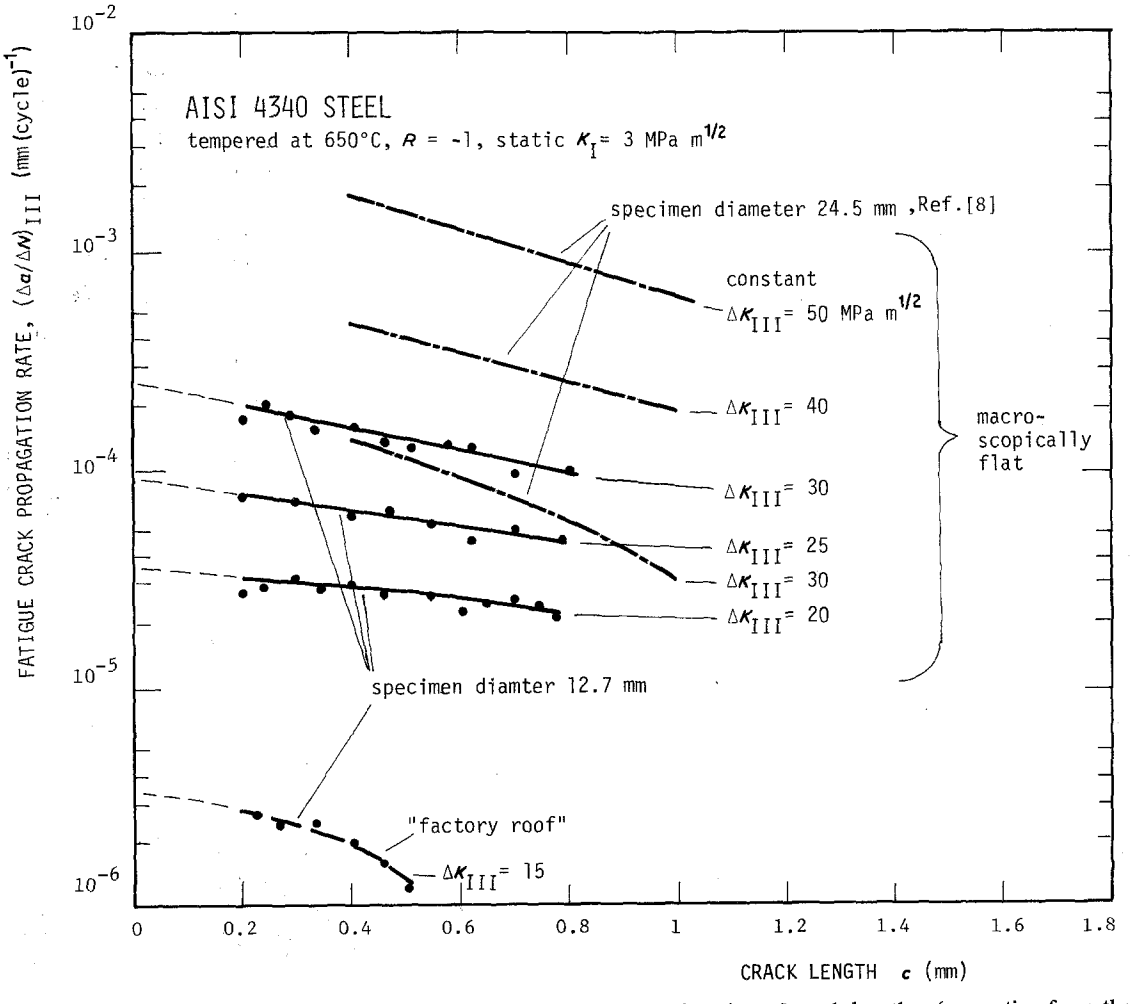

Figure 6 Comparison of fatigue crack growth rates in Mode III as a function of crack length c (emanating from the notch root) for 12.7 mm and 24.5 mm diameter specimens stressed at constant ΔK_{IIInom} values.

growth rates without "Mode III crack closure" influence are obtained [8]. In this case, $\Delta K_{\text{IIInom}} = \Delta K_{\text{IIIeff}}$. The extrapolated values of constant $\Delta K_{\text{IIInom}} = 30\,\text{MPa}\,\text{m}^{1/2}$ for the 12.7 mm and 25.4 mm specimens are in good agreement; however, at a crack length of 0.8 mm, the curves deviate approximately 50% from each other. Beside an increase in "Mode III crack closure" influence with growing crack length, this also indicates the growing influence of the greater shaft diameter.

In order to compare the fatigue crack growth behaviour in Mode III and Mode I stressing, the extrapolated $(\Delta c/\Delta N)_{\text{III}}$ values were plotted with fatigue crack growth values $(\Delta c/\Delta N)_{\text{I}}$ of [16] as a function of $\Delta K_{\text{I, IIIeff}}$ (Fig. 7). The extrapolated values that were obtained from 12.5 mm and 24.5 mm [8] diameter specimens lie on a straight line which is above the Mode I curve and show a greater slope (macroscopically flat fracture mode).

From the fractographic examinations it follows that, because of the torsion loading, initiation and propagation of branch cracks (see Fig. 2) in Mode I and Mode III + II begins. Consequently it is noted that a competition between the Mode III mean crack and the different branch cracks occurs [6, 8]. The outcome of this competition determines the macroscopic fracture mode.

Since the change of fracture mode from macroscopically flat to "factory roof" takes place with approximately identical crack growth rates on the mean Mode III crack and the branch cracks in Mode I, it is assumed that the ΔK_{I} for the branch cracks at the tip of the mean crack and the ΔK_{IIIeff} (mean) values must be of approximately the same magnitude.

After [8], the "Mode III threshold" value is taken to be that for which the fracture mode changes from Mode III (macroscopically flat) to Mode I (factory roof). According to the current investigation, it lies between 12 and 16 $\text{MPa}\,\text{m}^{1/2}$.

In Fig. 8, the crack growth increment per cycle in Mode I and III is plotted as a function of $\Delta\text{CTD}_{\text{I, III}}$. The Mode III curve shows a greater

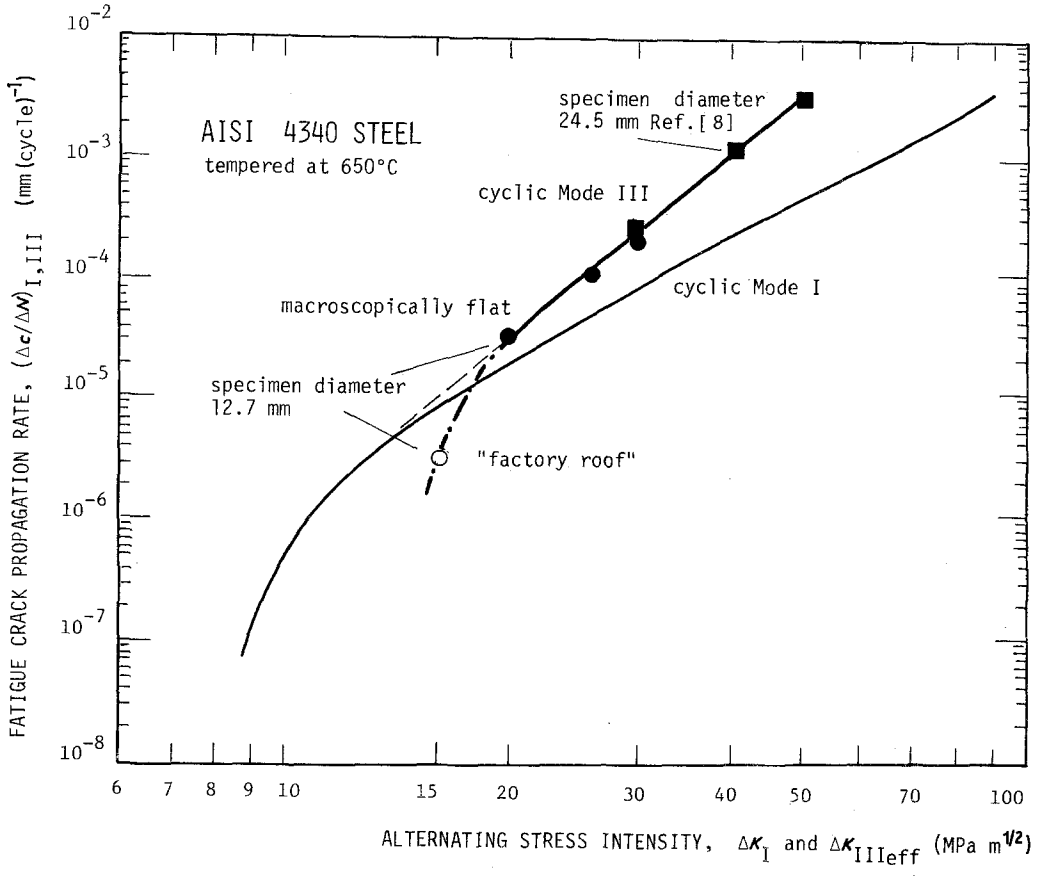

Figure 7 Comparison of fatigue growth rates in Mode I and Mode III as a function of ΔK_{I} and ΔK_{IIIeff}. Mode III values obtained through an extrapolation procedure from Fig. 6.

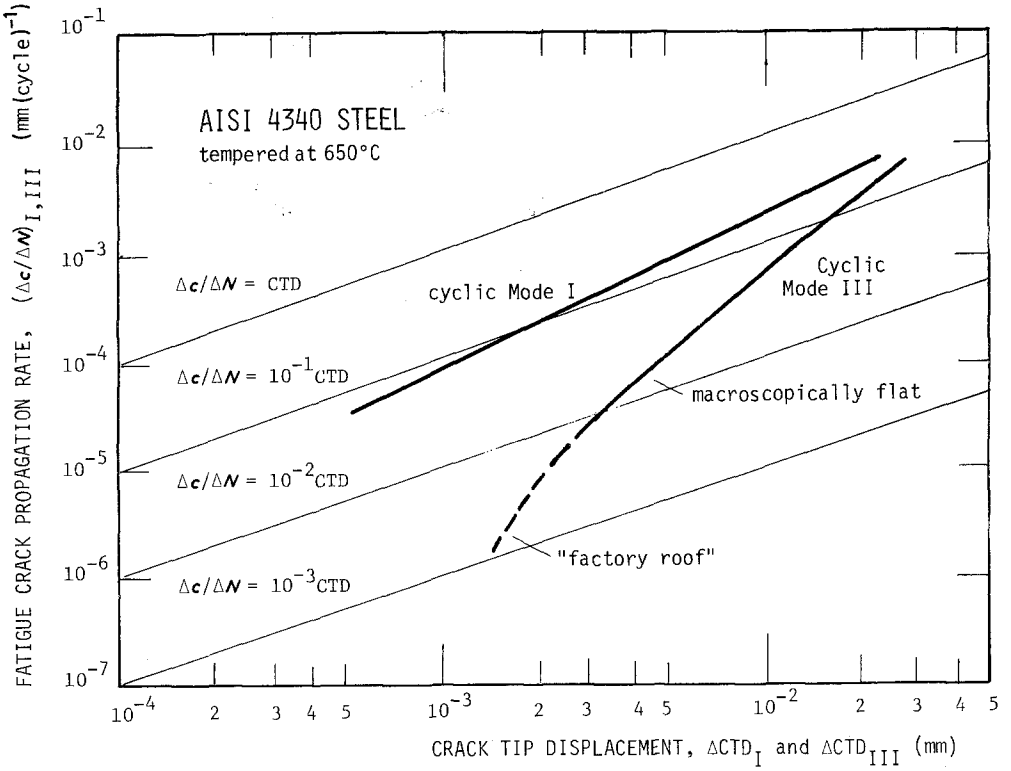

Figure 8 Variation of Mode I and Mode III fatigue crack growth rates as a function of ΔCTD_I and ΔCTD_{III}.

slope and lies below the Mode I curve for values of $\Delta CTD_{III} < 3 \times 10^{-2}$ mm.

Similarly to the well known dependence of Mode I crack growth rates on ΔK_I and ΔCTD_I, the crack growth rates for Mode III fatigue can be correlated by

$$(\Delta c/\Delta N)_{III} = A(\Delta K_{IIIeff})^m \quad (1)$$

$$(\Delta c/\Delta N)_{III} = B(\Delta CTD_{III})^n \quad (2)$$

For the linear part of the Mode III crack growth curve in Figs. 7 and 8, the parameters in Equations 1 and 2 have been calculated and lead to:

$$(\Delta c/\Delta N)_{III} = 2.7 \times 10^{-11}(\Delta K_{IIIeff})^{4.8} \quad (3)$$

$$(\Delta c/\Delta N)_{III} = 74(\Delta CTD_{III})^{2.4} \quad (4)$$

where $\Delta c/\Delta N$ is in mm(cycle)$^{-1}$, ΔK_{III} is in MPa m$^{1/2}$ and ΔCTD_{III} is in mm.

4. Discussion

The plastic zone of Mode III loading is several times larger than that for Mode I for similar materials and at the same stress intensity values. Compared with Mode I investigations it is therefore more difficult for small specimen dimensions in Mode III to fulfill the small scale yielding criterion that is required for the validity of the equations in Table III. For a stress intensity of 15 to 30 MPa m$^{1/2}$, plastic zone sizes are between 0.06 to 0.2 mm. For the higher growth rates, data have therefore been obtained under conditions of appreciable, but contained, yielding.

The application of fracture mechanics to short cracks is limited as well. For the Mode I case, the micro-mechanics of crack initiation and early growth of AISI 4340 tempered at 620°C were studied by Lankford [17]. It was found that for crack lengths greater than approximately 60 μm, the cyclic growth can be described using the formalism of fracture mechanics. In view of this, the smallest crack length observed in this study, 0.2 mm, can be safely used in fracture mechanics calculations.

During the measurements, the specimen is stressed by an axial load, so that a constant static K_I value of 3 MPa m$^{1/2}$ results at the crack tip. This value is only 1/2 of the ΔK_{Ith} value, and moreover of $CTD_I/\Delta CTD_{III} \approx 10^{-3}$ to 10^{-2}. It is assumed therefore, that an axial load as small as this has no influence on the Mode III fatigue crack growth rate. However, at present there are Mode III crack propagation studies underway to

investigate the influence of an axial load on soft materials [18].

The admissibility of an extrapolation to the non-realistic crack length $c = 0$ was discussed in [8]. It is justifiable on account of the linear behaviour of the measured curves (for a crack length greater than 0.2 mm) in Fig. 6, to consider the extrapolated growth rates as acceptable estimated values. These crack growth rates without a "Mode III crack closure" influence represent on the one hand an important possibility for the examination of crack growth rate models that do not consider rubbing fracture surfaces, and on the other hand give the maximum possible fatigue crack growth rates which incorporate a significant safety factor for use in engineering practice.

The great effect that is created by the "Mode III crack closure" influence on the crack growth rate in Mode III is shown by a comparison of these results and the studies of [5] on the same as well as [6] on En 16 steel (ultimate tensile strength, UTS, 972 to 1690 MPa). In [5, 6], the crack growth rates at a crack depth of 2 to 4 mm were measured. If the crack growth rates based on $\Delta K_{\mathrm{IIInom}}$ by [5, 6] are compared with the crack growth rates of $\Delta K_{\mathrm{IIIeff}}$ of this investigation at the same stress intensity range of 20 to 50 MPa $m^{1/2}$, then the crack growth rates of [5] are about a factor of 15 to 20 smaller, and for the crack growth rates of [6] about a factor 20 to 60 smaller.

In Fig. 6, the effect of the "Mode III crack closure" influence can also be estimated for different specimen diameters. For the 25.4 mm diameter specimens of [8], loaded with $\Delta K_{\mathrm{IIInom}} = 30\,\mathrm{MPa}\,m^{1/2}$, the crack growth rate amounts to only one fifth of the value for $c = 0$ at a crack depth of 0.8 mm. At a specimen diameter of 12.7 mm, this reduction amounts to only one half of this value at the same crack depth. The "Mode III crack closure" influence diminishes with decreasing shaft diameter; this is an important result requiring further discussion.

It is assumed that the Mode III fracture surface roughness is dependent on the material itself and on the applied $\Delta K_{\mathrm{IIIeff}}$ value but not on the specimen diameter. When such rough areas are approximated by inclined planes, surface pressures during torsional loading result in sliding of the inclined planes, and crack openings in direction ($\Delta \mathrm{CTD_I}$) [2]. Depending on the magnitude of the surface pressure at the inclined planes, local plastic deformation and the production of debris occur by abrasion. Estimation of the surface pressure was made for both specimen diameters at the same crack depth of 1 mm and with the same crack opening displacement ($\mathrm{CTD_I}$ evoked by inclined planes). The surface pressure for the small diameter specimen was found to be 40% less than that for the large diameter specimen. Thus we can understand why the "Mode III crack closure" influence will be weaker and the result in less production of debris for the 12.7 mm specimens than for the 24.5 mm specimens [8]. Further, we can state that production of abrasion debris and the difficulty of removing it from the crack will act effectively to increase the "Mode III crack closure". Taking this into account, as well as the strong dependence of the Mode III crack propagation on crack depth, specimen diameter, history, etc. the results of [2, 5, 6] must be carefully interpreted.

For the differing behaviour of crack growth rates of Mode III compared to Mode I, as shown in Figs. 6 and 7, a rough explanation of the observation can be given. In Mode I straining at larger crack openings, crack blunting takes place, diminishing the strain concentration at the crack tip. This is not the case with Mode III. The crack stays closed during stressing, and crack blunting does not occur to the same extent as in Mode I in ductile material. This probably contributes to the observed greater crack growth rates in Mode III than in Mode I for equivalent stress intensity levels and the greater slope of the Mode III crack growth curve. Rewelding processes, surely, occur at the crack tips during fatigue crack growth. This will probably result in a closed crack during loading in Mode III and reduce the crack length advance per cycle somewhat. Scientific investigations of these processes in Mode III fatigue crack growth have not been published to the author's knowledge.

Similarities in the crack growth behaviour in Mode III and Mode II, such as a closed crack during stress and the absence of crack blunting may be occurring. Otsuka *et al.* [19] found an approximately ten times higher fatigue crack growth rate in 7075-T6 and 2071-T4 aluminium in Mode II loading than in Mode I loading at equal stress intensities. If the Mode II stress intensity level falls below a certain value, a transition to Mode I crack growth will occur. In contrast to this, in mild steel they found that at higher ΔK_{II} levels the Mode I fracture dominated and at lower ΔK_{II} levels, the shear fracture mode was prevalent.

Pook and Greenan [20] studied Mode II fatigue crack growth behaviour in mild steel in the threshold region. They found that the threshold value for Mode II is controlled by the initiation of branch cracks in Mode I.

The change in fracture mode in Mode III (and probably in Mode II) results from the initiation, formation, and propagation of branch cracks [6, 8, 20]. Therefore, in the following, different mechanisms which lead to a change of the fracture mode are discussed.

In the plastic zone, microcracks are created during plastic deformation at matrix inhomogeneities (i.e. inclusions, grain boundaries). If such microcracks are advantageously oriented, they will be enlarged by the cyclic torsional loading. If the fatigue crack propagation rate for the branch crack is greater than that for the main cracks, the branch cracks will determine the fracture mode. Tipnis and Cook [21] have investigated the influence of inclusions on the flow and fracture behaviour in low carbon steel in torsion. They found that for the crack initiation and early crack growth in ductile fracture, the inclusions play the decisive role. Ritchie *et al.* [5] have presented a fatigue crack growth model based on the mechanism that crack advance is considered to take place by a Mode II coalescence of cracks, initiated at inclusions ahead of the main crack front. Also a relation between $(\Delta c/\Delta N)_{III}$ and ΔCTD_{III} was developed, with which they could verify the experimentally discovered crack growth rates based on nominal values.

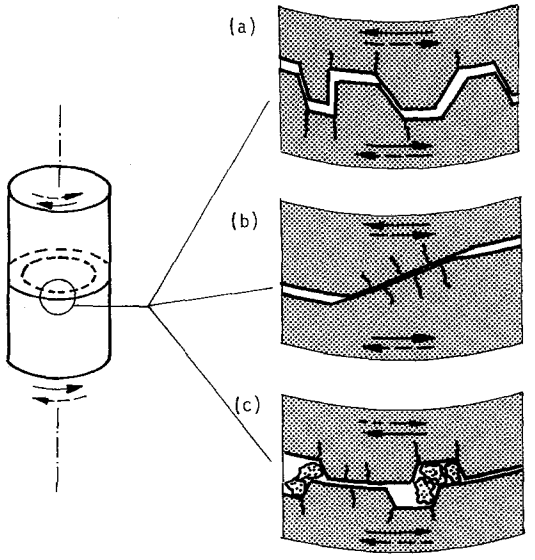

Figure 9 Schematic representation of mechanisms for branch crack initiation (a) mutual support, (b) fretting fatigue and (c) mutual support of debris.

Through the rubbing of crack surfaces in Mode III fatigue crack growth, crack initiation and propagation of branch cracks can result from mutual support of inclined surfaces (Fig. 9a); fretting fatigue [15, 25] (Fig. 9b); and mutual support of debris (Fig. 9c). In an investigation by Duquette [26] it was found that with a surface pressure of 41 MPa and a slip amplitude of 3 to 30 μm, approximately 10^5 cycles were required to failure. In mode III fatigue crack growth, such values certainly occur near the crack tip and fretting fatigue branch cracks can be initiated.

Pook [23, 24] developed criteria for the formation and propagation of Mode I branch cracks derived from Mode II or Mode III mean cracks. For the Mode III case, it was established that K_I (branch) = $0.74K_{III}$(main). This was used to determine the ratio of threshold values in Mode I and Mode III; the value found was $\Delta K_{Ith}/\Delta K_{IIIth} = 0.74$. In [24], this result was examined experimentally in mild steel and found to be in good agreement.

We cannot yet clearly decide which of the mechanisms are responsible for the fracture mode change because of the complex and not fully researched phenomena associated with it. Preliminary results [18] indicated that in materials of lower strength, containing inclusions (after Tipnis and Cook), microcracks initiated near inclusions are decisive. However, with materials with higher strength levels mutual support and fretting fatigue could be the initiation mechanism. For propagation of Mode I branch cracks, the considerations of Pook [23, 24] are applicable.

We conjecture the following basis for the change in fracture mode in this study. The material contained inclusions, i.e. manganese sulphide and calcium aluminate (size about 10 μm). Such inclusions can be the initiation point for branch cracks with different orientation. At higher Mode III stress intensity levels, branch cracks of Mode III + II grow more quickly than Mode I branch cracks, and a macroscopically flat fracture develops. At lower Mode III stress intensity levels, fatigue crack growth rates of Mode I cracks are higher; thus the Mode I branch cracks develop preferentially at approximately 45° to the specimen axis and a "factory roof" fracture occurs.

The extent to which a stress in the axial direction can influence the fracture mode change and

thus the "Mode III threshold" value must be the subject of further investigations. It would also be of interest to determine the influence of a presence of compressive residual stress on the fracture mode change.

5. Conclusions

Fatigue crack growth tests were conducted under cyclic torsion conditions ($R = -1$, 1 Hz test frequency) using AISI 4340 steel specimens with 12.7 mm diameter and with circumferential notches. The following are the conclusions derived from this investigation.

1. By a procedure of extrapolation which eliminates the influence of the "Mode III crack closure", Mode III fatigue crack growth rates higher than those at the same stress intensity level for Mode I were obtained with macroscopically flat fracture features. The slope of the Mode III fatigue crack growth curve is greater than that for Mode I.

The fatigue crack growth behaviour in the range of $\Delta K_{\mathrm{IIIeff}} = 18$ to 50 MPa $m^{1/2}$, having $\Delta \mathrm{CTD}_{\mathrm{III}} = 3 \times 10^{-3}$ to 2×10^{-2} mm can be characterized by the following equations:

$$(\Delta c/\Delta N)_{\mathrm{III}} = 2.7 \times 10^{-11} (\Delta K_{\mathrm{IIIeff}})^{4.8}$$

$$(\Delta c/\Delta N)_{\mathrm{III}} = 74 (\Delta \mathrm{CTD}_{\mathrm{III}})^{2.4}$$

2. A change in fracture mode occurs near the point of intersection of the Mode I and Mode III fatigue crack growth curves. The change of fracture modes is probably initiated by branch cracks which form at the inclusions in the plastic zone during the process of plastic deformation. At $\Delta K_{\mathrm{IIIeff}} < 18$ MPa $m^{1/2}$, the Mode I branch cracks which occur at approximately 45° to the specimen axis, grow faster than the Mode III crack and lead to a "factory roof" fracture. For $\Delta K_{\mathrm{IIIeff}} > 18$ MPa $m^{1/2}$, the Mode III + II branch cracks dominate the crack growth in the longitudinal and transverse planes of the specimen and a macroscopically flat Mode III fracture occurs.

3. A comparison of the "Mode III crack closure" influence at specimen diameters of 12.7 mm (described in this study) and of 24.5 mm [8] shows that this influence is not only dependent on the crack depth but also on the diameter of the specimen. The extrapolated crack growth rates show good agreement for the different specimen diameters.

Acknowledgement

This work was carried out during a sabbatical stay at the Massachusetts Institute of Technology from September 1980 to September 1981. The author thanks Professors A. S. Argon, F. L. McClintock and R. O. Ritchie for making possible this work and for helpful discussions, for which I also thank Professor C. Laird and W. Moffatt. Thanks are due to E. M. Babcock for helping to prepare this report. A research fellowship awarded by the Max Kade Foundation, New York, made the stay at MIT possible and is much appreciated.

References

1. E. K. TSCHEGG, Research Note, Massachusetts Institute of Technology, February 1981.
2. E. K. TSCHEGG, R. O. RITCHIE and F. A. McCLINTOCK, *Int. J. Fatigue* **5** (1983) 29.
3. H. NAYEB-HASHEMI, F. A. McCLINTOCK and R. O. RITCHIE, *Met. Trans.* **13A** (1983) in press.
4. H. NAYEB-HASHEMI, PhD thesis, Massachusetts Institute of Technology (1982).
5. R. O. RITCHIE, F. A. McCLINTOCK, H. NAYEB-HASHEMI and M. A. RITTER, *Met. Trans.* **13A** (1982) 101.
6. N. J. HURD and P. E. IRVING, in "Design of Fatigue and Fracture Resistant Structures", ASTM STP761, 212, (1982) American Society for Testing and Materials, Philadelphia, PA, 1981.
7. R. P. WRIGHT and R. A. QUEENEY, *Int. J. Fatigue* **4** (1982) 27.
8. E. K. TSCHEGG, *Mater. Sci. Eng.* **54** (1982) 127.
9. M. A. RITTER and R. O. RITCHIE, *Fat. Eng. Mater. Struct.* **4** (1982) 91.
10. M. A. RITTER, SM thesis, Massachusetts Institute of Technology, Dept. of Mech. Engineering, Cambridge, MA (1980).
11. H. TADA, P. C. PARIS and G. R. IRWIN, "The Stress Analysis of Cracks Handbook" (Del Research Corp., Hellertown, PA, 1973) p. 27.1–3.
12. J. R. RICE, in "Fracture: An Advanced Treatise" Vol. 2, edited by H. Liebowitz (Academic Press, New York, NY, 1968) p. 248.
13. C. F. SHIH, *J. Mech. Phys. Solids*, **29** (1981) in press.
14. H. NAYEB-HASHEMI, private communication (October 1980).
15. R. B. WATERHOUSE, in "Corrosion Fatigue", edited by A. J. McEvily and R. W. Staehle (National Association of Corrosion Engineers, Storrs, 1972).
16. J. T. TOPLOSKY, SM thesis, Massachusetts Institute of Technology, Dept. of Mech. Engineering, Cambridge, MA (1979).
17. J. LANKFORD, *Eng. Frac. Mech.* 9 (1977) 617.
18. E. K. TSCHEGG, *Mater. Sci. Eng.* in press.
19. A. OTSUKA, K. MORI, T. OHSHIMA and S. TSUYAMA, ICF5, Advances in Fracture Research, edited by D. Francois, Cannes, France, 1981, p. 1851.

20. L. P. POOK and A. F. GREENAN, in "Fracture Mechanics", ASTM STP 677 (American Society for Testing and Materials, Philadelphia, PA, 1979 p. 23.
21. V. A. TIPNIS and N. H. COOK, *J. Basic Eng., Trans. ASME Ser. D* **89** (1967) p. 533.
22. F. A. McCLINTOCK and R. O. RITCHIE, Proceedings of the ASME Winter Annual Meeting, edited by T. Mura, American Society for Mechanical Engineers, New York, NY, 1981.
23. L. P. POOK, in "Proceedings of the European Congress on Fracture III", edited by J. C. Radon (Pergamon Press, Oxford, New York, Toronto, 1980) p. 143.
24. L. P. POOK and J. K. SHARPLES, *Intl. J. Fract.* **15** (1979) R 223.
25. R. B. WATERHOUSE, in "Fundamentals of Tribology", edited by N. P. Suh and N. Saka (MIT Press, Cambridge, MA) p. 567.
26. D. J. DUQUETTE, in "Proceedings of the ICSMA 5, Strength of Metals and Alloys", Aachen 1979, edited by P. Haasen, V. Gerold and G. Kostorz (Pergamon Press, Oxford, New York, Toronto, 1979) p. 213.

Received 5 July
and accepted 13 September 1982